JCSE The Journal of Corrosion Science and Engineering
ISSN 1466-8858 Volume 14, Preprint 1 submitted 5 January 2011

# Effect of Microstructure on Corrosion Resistance of Pipelines Steels Buried in Alkaline Soil

Souad Brick Chaouche*

Laboratory Research Methods of Industrial Engineering-Environment
Faculty of Mechanical Engineering and Process Engineering
USTHB BP. 32 - EL ALIA 16110 BAB EZZOUAR ALGER – ALGERIA
brick_chaouche@hotmail.com
*Corresponding author

Azzedine Lounis

Laboratory Science and Engineering Materials
Faculty of Mechanical Engineering and Process Engineering
USTHB BP. 32 - EL ALIA 16110 - BABEZZOUAR - ALGER – ALGERIA
zlounis@yahoo.com

Ghania Nezzal

Laboratory Research Methods of Industrial Engineering-Environment
Faculty of Mechanical Engineering and Process Engineering
USTHB BP. 32 - EL ALIA 16110 - BAB EZZOUAR ALGER – ALGERIA
ghania.nezzal@enp.edu.dz
Fax : ++213 21 52 29 73.

**Abstract**
In this work, we tried to examine the effect of microstructure of Low Carbon pipeline steels on their behavior to corrosion when they are buried in alkaline soil. In this environment, the corrosion rate of these steels depends on a number of different parameters. Perhaps the most significant of these parameters, namely, is the formation, evolution and nature of the corrosion products, which are deposited on the metal surface. The laboratory experiments realized from electrochemical measurements and characterization of corrosion products have shown that the microstructure influences the properties of the corrosion layers, such as morphology, proportion of the various chemical compounds, adherence of the film and the protective properties. The results obtained are striking, not only there was a difference in certain properties of corrosion layers, but also protective power is strongly affected.

**Keywords:** microstructure, low carbon steel, pipeline steel, corrosion rate, corrosion products, protective properties, alkaline soil.

ISSN 1466-8858 Volume 14, Preprint 1 submitted 5 January 2011

**Biographical notes:**

Souad Brick Chaouche obtained her Engineering degree in Process Engineering from the University of Saad Dahlab, Blida in 1996. She completed her Graduation Diploma in 2003. She is a PhD student working in 'the corrosion Behavior of carbon steels in conducting media' from University of Science and Technology Houari boumadiene. Since then, she has been working as same university .The research she is carrying out is mainly focused on the relation between propriety of materials and corrosion behavior.

Azzedine Lounis obtained his PhD in Chemical Nuclear Engineering at the Faculty of Chemistry, University of Houari Boumedien in 1996. He also obtained a Graduation Diploma in Engineering Chemistry from the Polytechnic School (Algeria) in 1976, and a Master's degree from the Center of Science and Technology Nuclear, Algiers in 2003. His area of research includes Treatment of effluent (membrane technology: electrodialysis, micro /ultrafiltration), Industrial Maintenance, Material degradation (corrosion, electrochemistry, degradation of polmères), Porous and micrporeux Materials, Synthesis of membrane.

Ghania Nezzal is a Professor / Associate Director of Research of at University of Houari Boumedien, Algiers; she obtained her engineering degree (Chemical Engineering option) from the National Polytechnic School in 1966. She received her diploma from Dr. Engineer (Physics option) at the University of Algiers in 1972. She has obtained graduate Dr. Es Sciences at the University Claude Bernard Lyon I (France) in 1981. Her current positions: Professor at the University of Science and Technology Houari Boumadiane, Director of Laboratory Research in Process Engineering and Environment, Director of Research Associate., Director of the National Polytechnic School since April 2005. Her area of research includes: Electrochemical reactors / generators electrochemical energy, Separation Processes / Water Treatment / Desalination Water, Pollution / Environmental Protection / Sustainable Development, Training, Education - Language. She has published more than 65 articles in journals and conference proceedings.

## 1. Introduction

Carbon steels used in oil and gas transport, are manufactured according to the American Petroleum Institute (API) specification 5L and doesn't have a closely specified elemental composition and microstructure. Consequently, they are fabricated for a set of mechanical requirements such as yield strength, tensile strength and fracture toughness. This can allow for significant variations of the elemental composition and microstructure, which can also influence corrosion performance (API, 1995). Generally, the final microstructure and mechanical properties of carbon steel pipes are determined by its chemical compositions and thermomechanical treatments used during the production processes. Similarly, they can vary significantly between pipes of the same grade from different manufacturers, and these

ISSN 1466-8858 Volume 14, Preprint 1 submitted 5 January 2011

variations can lead to substantial differences in the corrosion resistance. When they are buried in the soil, these pipes are, generally, protected from the external aggressions by a bituminous coating whose action is coupled with a cathodic protection system. Unfortunately, corrosion and cracking problems still can occur in the system under certain conditions. The corrosion rate of these pipes varies according to a host of different parameters. However, the most Significant of these parameters is the formation, evolution and nature of the corrosion products which are deposited on the metal surface.

The influence of layer of corrosion products on the steel corrosion is through a physical blocking effect that inhibits the access of corrosive species; it can completely stop, or accelerate the corrosion process. Therefore, the nature of the layer of deposit is the main factor influencing the protection of steel. It was necessary to know more about the structure and properties of passive film. A considerable number of investigations have been devoted to the study of the electronic properties and chemical compositions of corrosion products, particularly, on steel (Nasu et al, 2002; Chang et al, 2005; Samide et al, 2004; Wan et al, 2003;). Others have studied the effect of various parameters such as pH, oxygen levels, humidity, composition of the electrolyte on the mechanism formation and transformation of the oxides and hydroxides, particularly in soil (Freire et al, 2009; Benmoussa et al, 2009). But little works has addressed the influence of microstructure, on the formation of iron oxides, and on their inhibitory properties. In this work, we try to examine the microstructural effect, on the corrosion resistance of some grades of carbon steel when they are subject to corrosion in alkaline soil by the evaluation of the nature and properties of deposit layer formed on the surface of samples. In order to characterize the best resistance to corrosion of these grades steel, several electrochemical techniques were used, such as the polarization curves, weight-loss, polarization resistance, and electrochemical impedance spectroscopy (EIS). Fourier Transform Infrared spectroscopy (FTIR), Scanning Electron Microscopy (SEM), Energy

ISSN 1466-8858 Volume 14, Preprint 1 submitted 5 January 2011

Dispersive X-ray analysis (EDX), and X-ray diffraction (XRD) techniques were used to characterize the phase constituents of the rust and to deduce long-term corrosion behavior of steel.

## 2. Experimental part

### 2.1. *Samples preparation and metallurgical assessment*

The test samples were fabricated from pipes of API 5L X42, X52, X60, and X70 steel. The pipes are given by the national company of marketing and transport of petroleum (SONATRACH, Algeria). They come from different manufacturers, and they were subjected to different thermomechanical treatments. Therefore, it presents a noticeable difference in their microstructures. Materials have been chosen as representative of tubes posed on the line past ten years, where corrosion and corrosion cracks were detected. The quantitative and qualitative analyses of the samples were carried out by fluorescence of X-rays spectrometry (Philips XRF). Chemical compositions of samples were listed in Table 1. The samples, with an effective surface area of 1 $cm^2$, were firstly covered by epoxy resin, then polished on metallographic abrasive paper, and etched with Nital solution. Microstructure of samples was examined by optical microscopy type ZEISS equipped with a numerical camera (Nikon 500). Grains size Measurement and percentages of existent phases were determined using the software ATLAS (Zeiss) .The Vickers hardness tests were made by penetration, using a BUEHLER (Micronet 3).

**Table 1:** Chemical components of the steels used in the tests (W. %)

| grade | Cr | Ni | Mn | Si | Cu | Co | V | S | P | Ti | Al | Mo | Nb | C |
|---|---|---|---|---|---|---|---|---|---|---|---|---|---|---|
| X42 | 0.0022 | 0.0166 | 0.6797 | 0.2219 | 0.03143 | 0.0203 | - | 0.0036 | 0.0105 | 0.0025 | 0.0188 | 0.0363 | - | 0.1395 |
| X52 | 0.0032 | 0.0017 | 1.2888 | 0.1436 | 0.0215 | 0.0126 | 0.0563 | 0.0186 | 0.0015 | 0.0041 | 0.0399 | - | 0.0564 | 0.1740 |
| X60 | 0.0018 | 0.0011 | 1.0760 | 0.2334 | 0.0250 | 0.0220 | 0.0040 | 0.0023 | 0.0028 | 0.0022 | 0.0257 | 0.0011 | - | 0.1250 |
| X70 | 0.0054 | 0.0622 | 1.6648 | 0.3152 | 0.0213 | 0.0159 | 0.0665 | 0.0091 | 0.0089 | 0.0039 | 0.0343 | 0.0123 | 0.0321 | 0.1722 |

ISSN 1466-8858 Volume 14, Preprint 1 submitted 5 January 2011

2.2. *Soil solution*

The test solution was a soil-extracted solution (NS4), consisting of 483 mg/l $NaHCO_3$, 122 mg/l KCl, 181 mg/l $CaCl_2$, and 131 mg/l $MgSO_4.7H_2O$ (pH= 8.2). All the tests were performed at ambient temperature.

*2.3 Corrosion testing*

Electrochemical measurements were conducted in a three-electrode system. The reference electrode was saturated calomel electrode (SCE), the counter electrode was platinum (Pt), and pipe steel electrode was used as working electrode. EG&G model 273 potentiostat/galvanostat was used in polarization measurements. During polarization curve measurements, the potential scan rate was 20mV/min. The Ohmic potential drop was compensated by the instrument. EIS measurements were made of corrosion potential, applying a sinusoid signal with 10mV amplitude in a frequency interval from 100 kHz to 10 mHz. The impedance diagrams were obtained using a Versastat (model 1025) frequency response analyzer and an EG&G PAR 283 Potentiostat. To determine the corrosion rate by weight loss, the samples were prepared and weighed, then immersed in NS4 solution for 40 days. After removal of oxide layers formed on the surface by polishing and dissolution of traces of oxides, we measured the weight loss.

*2.4. Analysis of corrosion products*

The Scanning Electron Microscope (SEM) model XL 30S FEG coupled with Energy Dispersive X-ray analysis (EDX), was used to observe the surface morphology and determine the Elemental composition of corrosion products. In order to obtain a basic identification of the existent oxides, the corrosion products were analyzed by X-ray diffraction in the angular range of 0°-90° two-theta using Cu-Kα, a Siemens D500 diffractometer was used. The Fourier Transform Infrared spectra of corrosion products samples were recorded, after pressing the rust in the form of disc using spectroscopically pure KBr under vacuum at room temperature,

ISSN 1466-8858 Volume 2011

using a Nicolet Nexus 670. Spectrum analysis was realized in using the software Omnic 6.00.).

## 3. Results

### *3.1. Elemental composition*

Chemical analysis revealed that the elemental composition of the steel samples were similar, with the exception of Niobium, Molybdenum and Vanadium (Table 1). All samples did not contain the significant levels of Chromium, and Nickel. Phosphorus and Sulfur levels are well below the maximum limits set by the 5L specification. The X52 and X70 grade materials comprised notable levels of the grain-refining elements Niobium, Vanadium, Titanium, and Aluminum, which are also known to refine grain size. This refining of the grain size is desirable since it is the only structural change that concurrently increases both strength and toughness (Mc Gannon, 1971).

### *3.2. Microstructure*

It is important to note that the present phases are mainly determined by elemental composition, thermal and mechanical history (Higgins, 1993). The low carbon and alloy contents of steels suggest that they can be expected to have predominantly ferritic microstructures (Samuels, 1980). Figure 1 shows the various microstructures observed in this study. The microstructure of X42 (Figure 1a) has a ferrite/pearlite structure (pearlite dark areas, and ferrite white areas), and the pearlite phase is uniformly distributed. The X52 sample (Figure 1b) has a ferrite-pearlite microstructure, the grains size is finer compared to the X42. The X60 structure (Figure 1c) consists of ferrite and of pearlite, with a minor amount of bainite. The microstructure of X70 sample (Figure 1d) is consisted of the acicular ferrite, pearlite, and martensite. A very finer structure is observed, and no inclusion or pores are visible in this sample. Table 2 displays a summary of the various microstructure and mechanical properties of the steel samples.

JCSE The Journal of Corrosion Science and Engineering
ISSN 1466-8858 ed 5 January 2011

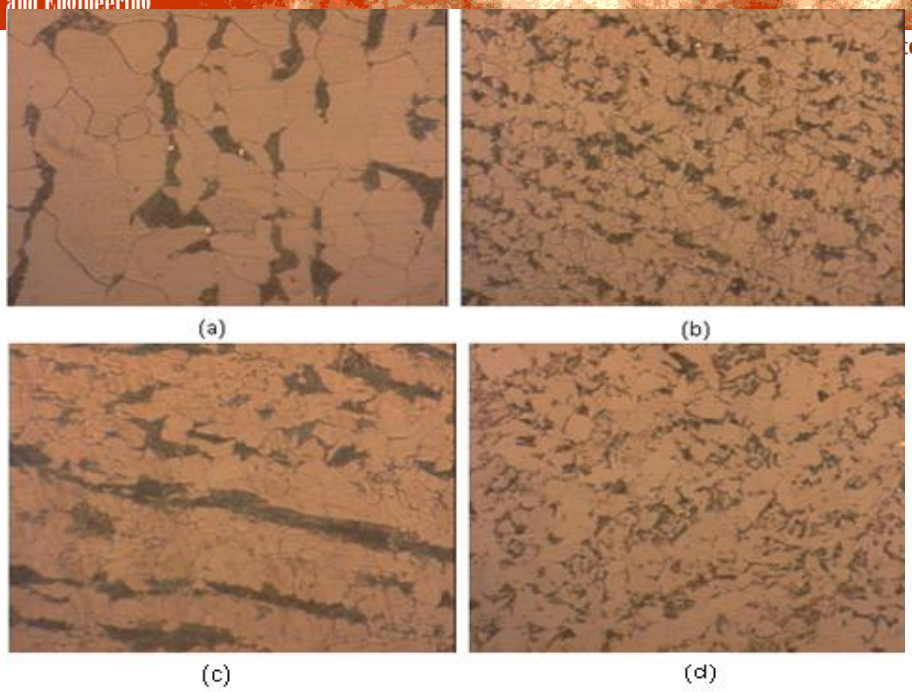


**Figure 1** Metallographic views of the microstructures of API 5L X42 (a), X52 (b), X60 (c), X70(d), (magnification 500 x)

**Table 2:** Summary of microstructures and hardness Values (VHN)

| grade | structure | % ferrite | % pearlite | grains size (µm) | Hardness 500gs |
|---|---|---|---|---|---|
| X42 | Ferrite/pearlite | 80.8 | 18.2 | 20 – 30 | 158 |
| X52 | Ferrite/pearlite | 71.6 | 27.5 | 5 – 10 | 195 |
| X60 | Ferrite/pearlite/bainite | 72.2 | 24.9 | 10 – 15 | 214 |
| X70 | Ferrite/pearlite/martensite | 73.8 | 24.7 | very fine | 288 |

*3.3. Polarization curves*

In the polarization curves (Figure 2), express the classical aspect of corrodible materials. Indeed, the corrosion current density increases with the imposed current, showing that the attack continues. The dissolution of X42, X52, X60 and X70 carbon steel is controlled by kinetics of pure activation (anodic curve). The stable passive region could not be developed on the four curves. Polarization parameter values; corrosion current density ($I_{corr}$), corrosion potential ($E_{corr}$), anodic and cathodic Tafel slope ($b_a$, $b_c$), and polarization resistance ($R_p$) are given in Table 3. The polarization resistance ($R_p$) was calculated using the Stern-Geary Equation (Stern and Geary, 1957):

$$Rp = \frac{ba\ bc}{(ba + bc)\ 2.3\ Icorr}$$

The comparing of the polarization resistance values (Table 3) shows that the samples have a different corrosion behavior. Indeed, it was noticed that the X42 steel has the best corrosion resistance (Rp highest) compared to other samples (X52, X60, and X70). This shows that the variation of corrosion behavior of pipe samples studied is probably related to differences in the microstructure.

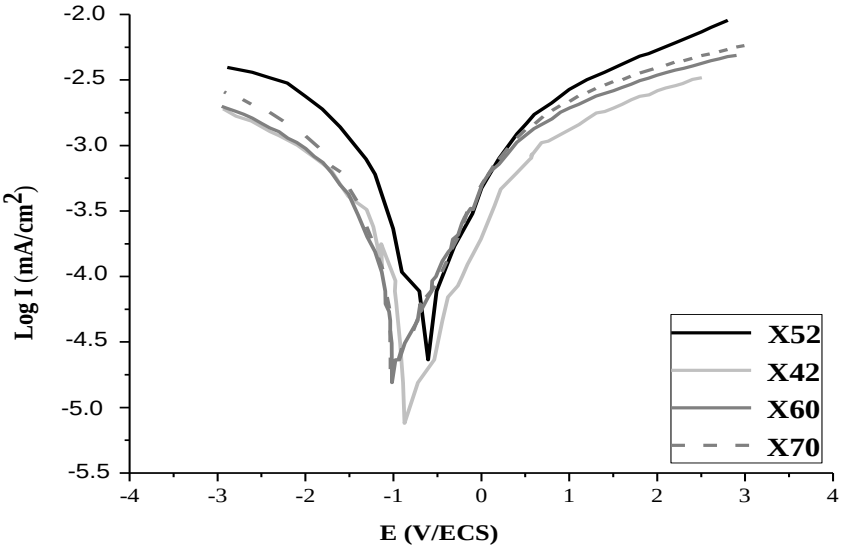


**Figure 2** Polarization curves of carbon steel in NS4 test solution of soil environment

**Table 3:** Polarization parameters for the corrosion of carbon steel in soil test solution

| grade | $E_{corr}$ (mV) | $I_{corr}$ ($\mu A/cm^2$) | $b_a$ (mV/dec) | $b_c$ (mV/dec) | $R_p$ ($\Omega.cm^2$) |
|---|---|---|---|---|---|
| X42 | - 697 | 0.450 | 233.33 | -250 | 3380.41 |
| X52 | -690.5 | 2.661 | 226.66 | -303.36 | 149.405 |
| X60 | -703.4 | 1.307 | 250 | -300 | 356.24 |
| X70 | -702 | 2.187 | 285.71 | -363.63 | 265.69 |

### *3.4. Corrosion rate results*

Corrosion rates of carbon steel samples measured by polarization resistance and weight-loss have been summarized in Table 4. The X42 steel sample presents the lowest corrosion rate compared with those of X60, X70 and X52. These reflect clearly the relationship between the microstructure of the material and its resistance to corrosion, and confirm the polarization curve results.

ISSN 1466-8858 Volume 14, Preprint 1 submitted 5 January 2011

**Table 4:** Corrosion rate of various carbon steel samples, measured by weight-loss, and polarization resistance

| grade | Weight-loss | | Polarization resistance | |
|---|---|---|---|---|
| | Δm (mg) | $V_{corr}$ (mmpy) | $R_p$ (Ω.cm$^2$) | $V_{corr}$ (mmpy) |
| X42 | 1.5 | 0.0175 | 7308.28 | 0.015219 |
| X52 | 39.7 | 0.4643 | 350.45 | 0.5116 |
| X60 | 19.4 | 0.2269 | 1067.73 | 0.28107 |
| X70 | 25.1 | 0.2935 | 789.33 | 0.33805 |

*3.5. EIS measurements*

When carbon steel specimen is placed in a specific medium (soil in our case) it is formed on metal surface, an irreversible interfacial reaction, which results in a layer of passivation or corrosion. This formation affects the charge-transfer and modifies the process of the corrosion of steel. The electrochemical impedance spectrometry (EIS) will enable us to separate the various contributions from the mechanisms of corrosion by their kinetics. The fast and slow phenomena are observed respectively at high and low frequency. In other words these electrochemical measurements of impedance will dissociate the solution resistance (Rs), charge-transfert resistance polarization (Rt) and the resistance of the deposits on surface (capacity of double-layer CHF). The Figure 3 shows the diagrams of Nyquist measured on the exposed surface of carbon steel samples in solution NS4. We note that there has a common feature for all EIS studies, the impedance curves are dominated with one time constant only, i.e, a semicircle over the high frequency range. However, the semi-circle diameter increased significantly when moving from finer microstructure to a coarse microstructure. The largest charge-transfer resistance was recorded for the X42 steel (2148 Ω.cm2), and the smallest semicircle for X52, the charge-transfer resistance is about 650 Ω cm². This decreasing resistance could be caused by the instability of the oxide layers or by the porosity. A porous layer of corrosion product deposit in defect will also contribute to the limited mass-transfer of oxygen (Zhong et al, 2008). The sizes of the semicircle measured on X60 and X70 steels were between these extremes. The Figure 3 shows that the diffusive impedance increases,

ISSN 1466-8858 Volume 14, Preprint 1 submitted 5 January 2011

indicating that diffusion of oxygen becomes more difficult for the X42 and X60 samples, and consequently a decrease in corrosion rate

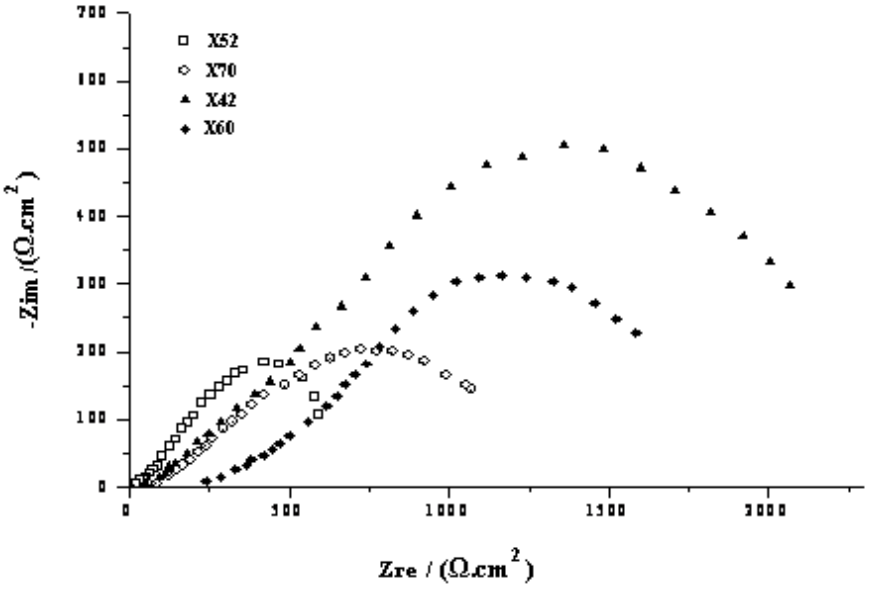


**Figure 3** Nyquist plots of carbon steel samples that immersed in NS4 soil solution

*3.6. Corrosion products characterization*

*3.6.1. SEM analysis*

Examination under a Scanning Electron Microscopy (SEM) of surface after the corrosion in NS4 soil solution will reveal on it the presence of corrosion products. The corrosion layers formed on the surface of samples exhibit very different morphology (Figure 4). On the X42 sample (Figure 4a), the layer is compact and uniformly covering the surface. While for X52, X60 and X70 (Figure 4b, 4c, 4d) corrosion products are porous and defective, or do not cover the entire surface. The corresponding energy spectrum (Figure 5) shows that these products are made of a number of chemical elements whose majority is iron and oxygen. From the peaks of iron, corrosion products consist principally of iron oxide. Indeed, the iron peaks are large indicating that the iron is not under an individual but it is combined with other chemicals, probably oxygen and hydrogen.

JCSE The Journal of Corrosion Science and Engineering
ISSN 1466-8858 Volume 14, Preprint 1 submitted 5 January 2011

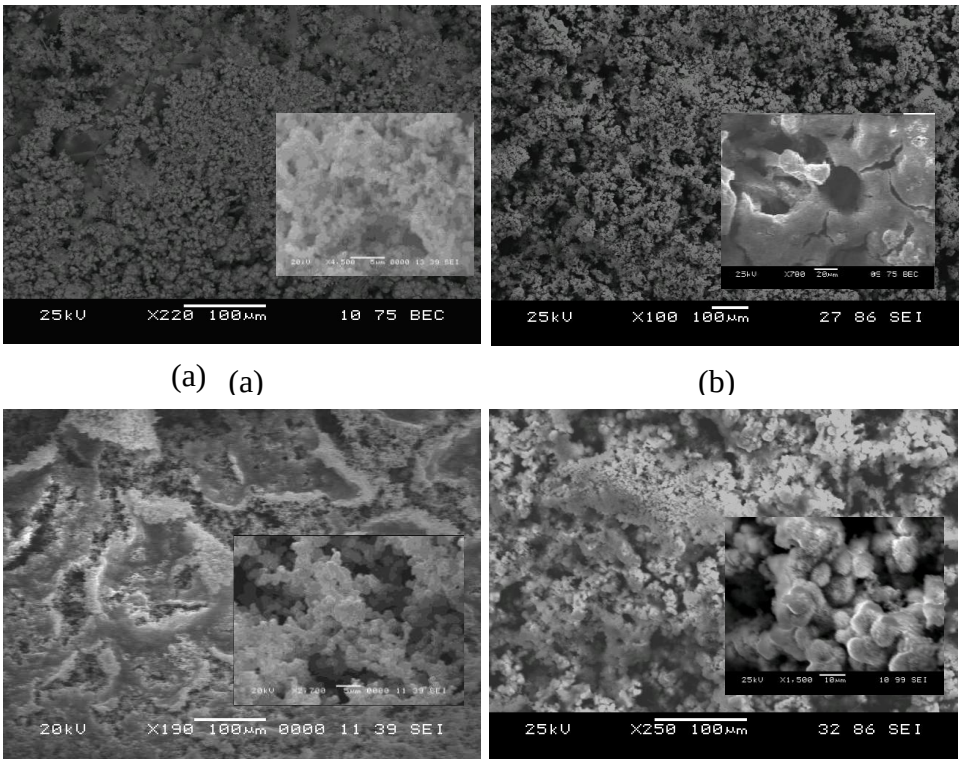


(a) (a) (b)

(c) (d)

**Figure 4 Surface** morphology of carbon steel samples exposed for ' to soil test solution: (a) X42, (b) X52, (c) X60, (d) X70

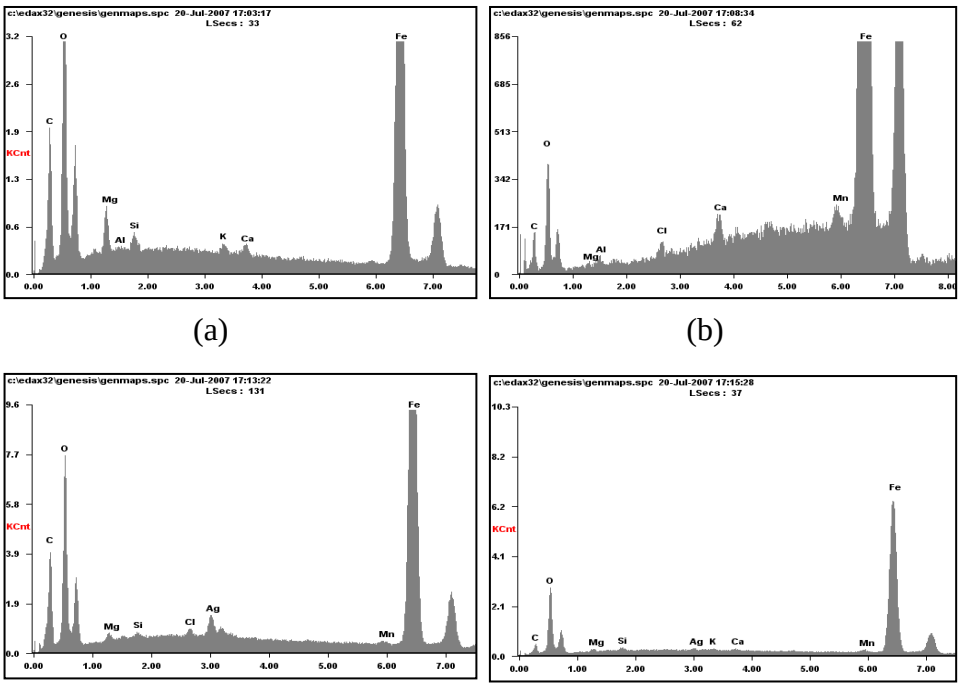


(a) (b)

(c) (d)

**Figure 5** The energy dispersive (EDX) spectra of corrosion products formed on carbon steel specimens: (a) X42, (b) X52, (c) X60, (d) X70

### 3.6.2. *FTIR characterization*

It can also be seen in Figure 6 that the FTIR spectra corresponding to different carbon steel samples were similar. The layers formed on the steel surfaces are composed of a mixture of goethite (α-FeOOH), lepidocrocite (γ -FeOOH), δ-FeOOH, and $Fe_2O_3$. Goethite had peculiar peaks at 885 $cm^{-1}$ and 780 $cm^{-1}$, and lepidocrocite had peaks at 1020 $cm^{-1}$, 750 $cm^{-1}$and 1450 $cm^{-1}$, while the amorphous δ-FeOOH had peaks at 1124 $cm^{-1}$ and 794 $cm^{-1}$. $Fe_2O_3$ had peculiar peaks at 466 $cm^{-1}$. The FTIR spectra of the relevant phases can be found in the literature (Raman et al, 1991; Misawa et al, 1974). The peak at 3120 $cm^{-1}$ is the O-H stretch vibration from lepidocrocite, and the peak at 3380 $cm^{-1}$ is the O-H stretch vibration from δ-FeOOH (Yamashita, 1994).

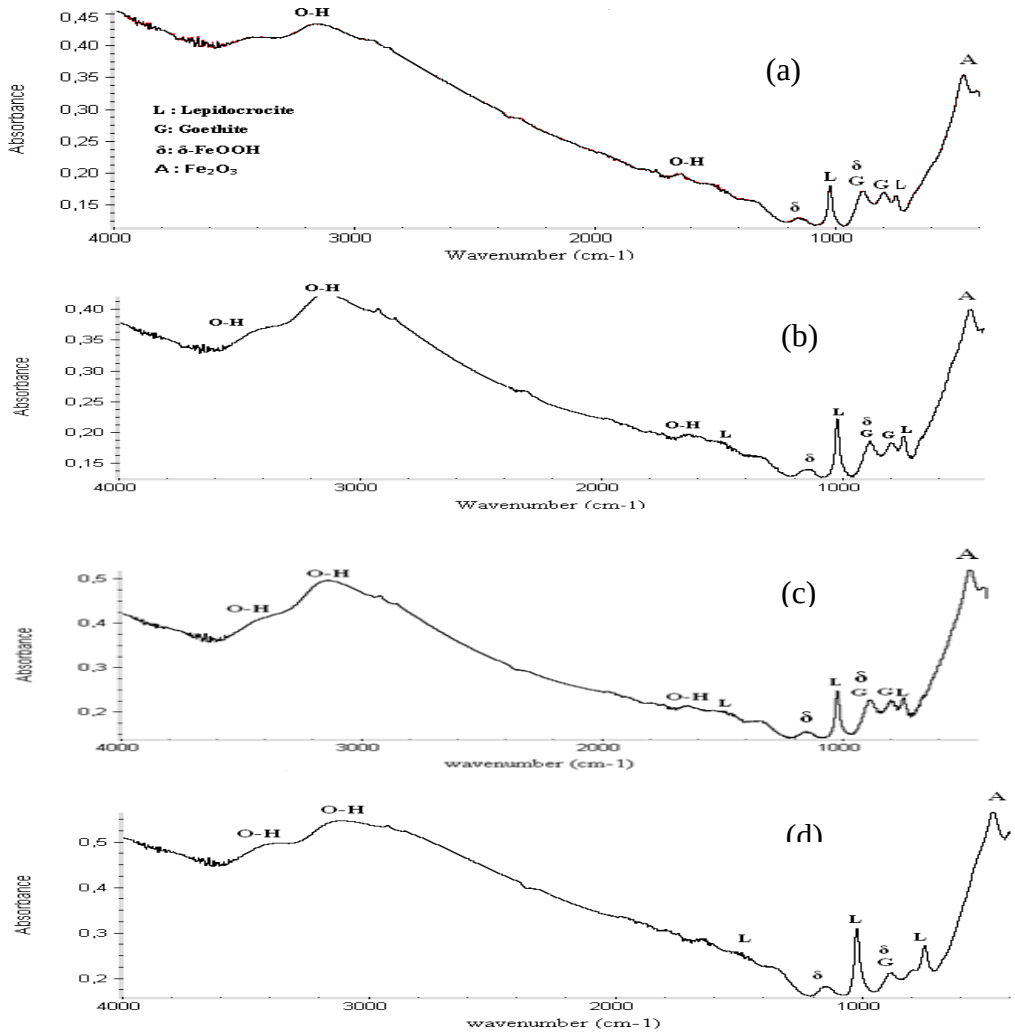


**Figure 6** FTIR spectra of the carbon steel samples corroded by NS4 soil solution during 40 days: X42(a), X52 (b), X60 (c), and X70 (d)

ISSN 1466-8858 Volume 14, Preprint 1 submitted 5 January 2011

*3.6.3. The XRD characterization*

The XRD data were used to support the FTIR spectra results. Standards for the XRD analyses were obtained from literatures (Misawa et al, 1974; Nishimura et al, 2000; Marco et al, 2000; Oh, 1999). The composition of corrosion products on the various steels determined by XRD analysis is shown in Figure 7.

According to the XRD analysis results, the rust mainly consisted of the following phases: goethite (α-FeOOH: Joint 290713), lepidocrocite (γ -FeOOH: JCPDS 80098), ferrihydrite ($Fe_2O_3$, H2O: JCPDS 290712). The peaks of δ-FeOOH were mixed with that of goethite and lepidocrocite in the XRD patterns, while the peaks of the three phases can be clearly identified in the FTIR spectra. In the case of X70, in addition to other oxides Fe (OH) 3 (JCPDS 380032) was detected.

It can be seen from the XRD patterns that goethite and lepidocrocite were the main constituents of rust layers, which are in agreement with the result from the FTIR spectra.

In the figure 7a, the relative intensities of goethite in rust layer of X42 sample are stronger and the diffraction peaks are broader than in the rust layer of samples X60, X70, and X52 (Figure 7b,7c, and 7d). This latter result indicates that the rust layer of X42 represent a smaller grain size. The Rust with a smaller grain size might be easy to form a more compact protective film and thus could hinder the permeation of water and oxygen more effectively, and retarded the corrosion of sample (Wan et al, 2004).

JCSE The Journal of Corrosion Science and Engineering
ISSN 1466-88[illegible] nitted 5 January 2011

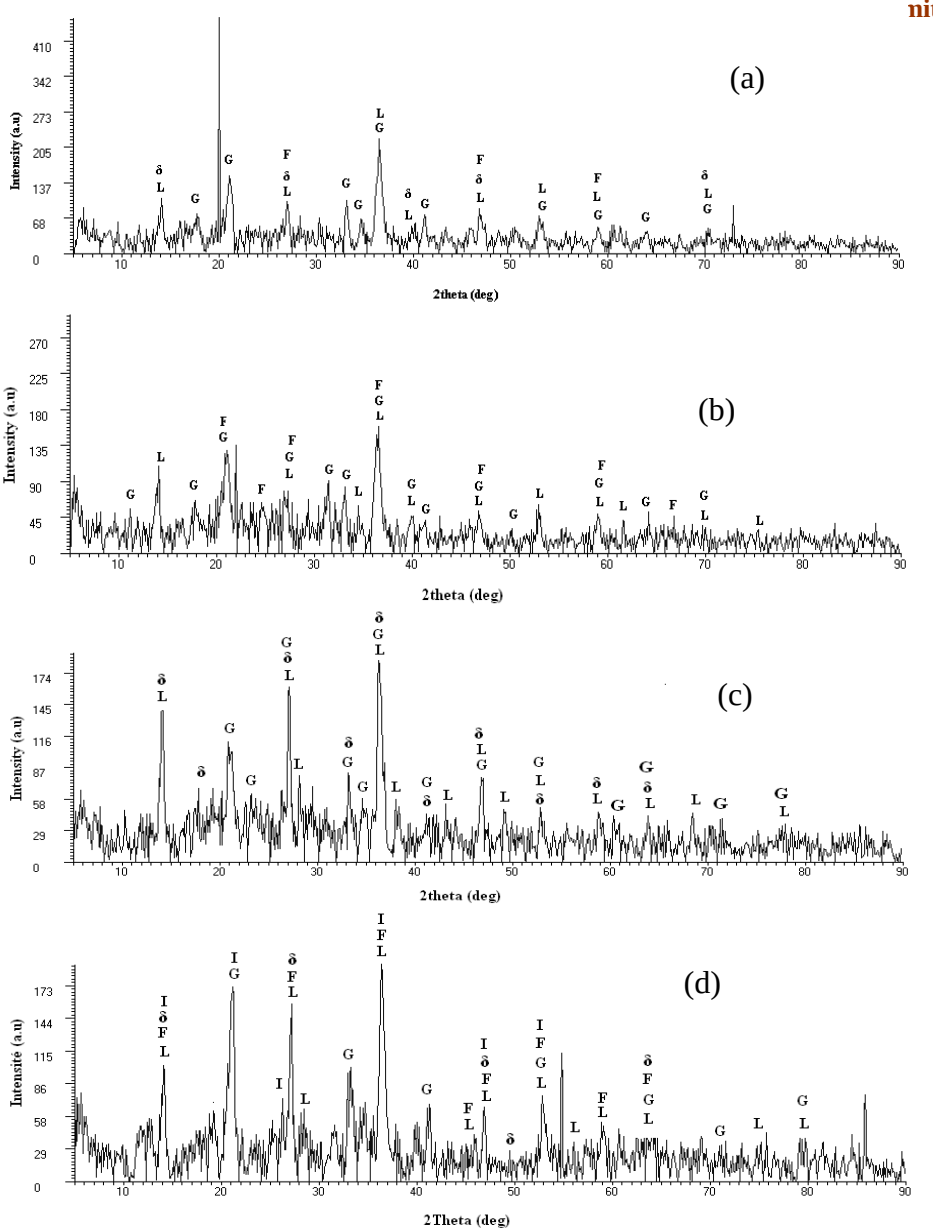


**Figure 7** XRD characterizations of corrosion products formed on surface steel samples after 40 days of test in soil solution: G: goethite, L: lepidocrocite, δ: δ-FeOOH, F: $Fe_2O_3$, I: $Fe(OH)_3$

## 4. Discussion

In the presence of an electrolyte such as water, corrosion reactions of low carbon steel are dominated by the Oxygen reduction and iron oxidation. In alkaline soil solution the corrosion mechanism of pipeline steel is more complex. The anodic process is described as a multiple-step oxidation reaction of iron with the formation of $Fe(OH)_2$, then FeOOH (Cheng, 1999; Tiana, 2008):

ISSN 1466-8858 Volume 14, Preprint 1 submitted 5 January 2011

$$Fe + H_2O \longrightarrow Fe(OH) + H^+ + e^- \quad \text{(Esq. 1)}$$

$$Fe(OH) \longrightarrow Fe(OH)^+ + e^- \quad \text{(Eq 2)}$$

$$Fe(OH)^+ + OH^- \longrightarrow Fe(OH)_2 \longrightarrow \text{Hydrous } Fe(OH)_2 \text{ layer} \quad \text{(Eq 3)}$$

$$Fe(OH)_2 \longrightarrow FeO + H_2O \quad \text{(Eq 4)}$$

$$4\,Fe(OH)_2 + O_2 + 2H_2O \longrightarrow 4Fe(OH)_3 \quad \text{(Eq 5)}$$

$$4\,Fe(OH)_2 + O2 \longrightarrow 2Fe_2O_3 + 4H_2O \quad \text{(Eq 6)}$$

$$Fe(OH)_3 \longrightarrow FeOOH + H_2O \quad \text{(Eq 7)}$$

XRD and FTIR results showed that all iron oxides, as suggested in Eq1-7, are possible in alkaline soil. These iron oxides exist on the steel surface as a deposited layer because only one time constant was measured on the EIS plots (Figure 3). Effect of the iron oxide deposit layer on steel corroded is mainly through a physical blocking effect (Cheng, 2005; Asher, 2007), which inhibits the access of corrosive species to the steel surface. Therefore, compactness of the deposit layer is a main factor that affects the protectiveness of the steel.

The corrosion products formed on the surface of the samples have almost the same chemical composition but different structures and morphology (Figure 4, 6 and 7). The compact and complete deposit layer formed on X42 steel (Figure 4a) would inhibit effectively the steel corrosion. This sample presented the lowest corrosion rate. However, the deposit layer formed on the surface of X52, X60, and X70 steel are porous and defective (Figure 4b, 4c, 4d), and does not effectively protect the steel. These samples have a very low resistance to corrosion compared to X42 steel (Table 3, Table 4). Therefore, the charge-transfer resistances measured on these steels are much lower than the X42 steel, as shown in (Fgure3). These results are in agreement with the XRD results.

During the corrosion process, the agglomeration of the hydroxyl ions ($OH^-$) is done in a continuous way around the ion metal and many works show that the ratio oxygen/metal is not whole and constant. On the one hand, the formed hydroxides are not defined compounds and

on the other hand the surface quality of the sample influences directly the speed of corrosion.

The surface offered by the substrate to the environment determines the sites where the attack occurs. Also let us note that their precipitation will be carried out differently. It follows that their products of solubility depend clearly on the crystalline forms and the way in which precipitation was carried out. Considering the obtained results, we can suggest that the steel microstructure affects the properties of oxide layers.

The use of new manufacturing processes and application of Heat treatment lead to change in the structure of carbon steels, and improves their mechanical properties. Recent studies have shown that these changes significantly affect their resistance to corrosion (Du et al, 2009; Bulger et al, 2006; Clover, 2005). In the case of samples of carbon steel studied in this work, manufacturing procedures have led to microstructures and properties differently (Figure 1 Table 2). The X42 steel structure with a large polyhedral grain (coarse) of ferrite-pearlite and with a lowest rate of pearlite has the greatest resistance to corrosion (0.015 mmpy). While the X52 steel characterized by ferrite / pearlite structure band, relatively fine grain and a high rate of pearlite, has the lowest corrosion resistance (0.512 mmpy). It was found that steels with a banded ferrite/pearlite structure present poorly performance in terms of corrosion resistance, and this can be attributed to a segregated distribution of the iron carbide phase cementite (Fe3C). This is consistent with suggestions made elsewhere that the shape and distribution of ferrite/Fe3C plays an important role in influencing the corrosion rate (Raman et al, 1991). X70 and X60 steels have a low resistance to corrosion (0.28107 mmpy, 0.33805 mmpy) compared to X42, but better compared to X52. X60 presents a structure ferritic-pearlitic with a minor amount of bainite, and X70 is consisted of the acicular ferrite, pearlite, and martensite with a very fine grain size. Insignificant differences were observed in the corrosion resistance of these steels.

ISSN 1466-8858 Volume 14, Preprint 1 submitted 5 January 2011

## 5. Conclusion

The present work shows that corrosion of steel is affected by its microstructure. The choice of a steel grade cannot be carried out only for these mechanical properties, but must take into account the corrosion resistance and the properties of the oxide layer that is formed when the pipe is buried in soil. This study has shown that the corrosion rates vary significatively between different carbon steels. Furthermore, the line pipe steels investigated in this paper revealed corrosion rate variations of 0.015 mmpy and 0.512mmpy. It has been shown that variations in the corrosion rate are partly due to differences in the microstructure. It was found that steel X42 with ferrite/pearlite structure with large grain size present better results in terms of corrosion resistance and this has been attributed to the rate of pearlite and grain size. By contrast, all other microstructural types have a poor corrosion resistance. The nature of corrosion products formed on metals is the ultimate factor which controls their corrosion behavior. According to our results, the microstructure affects the corrosion resistance of steel and leads to the formation of a deposit layer that can effectively protect the steel or accelerate the corrosion process. This paper has demonstrated that steel microstructure is an important consideration when selecting a grade pipe material for a particular application**.**

## References

American Petroleum Institute (1995), 'API Specifications 5L', 41st edn.

Nasu S., Kamimura, T., Tazaki, T. (2002), 'Characterization of Corrosion Products on Steel Surfaces' Hyperfine Interactions, Vol. 175, pp.139-140.

Samide, A., Bibicu, I., Rogalski, M. S., Preda, M. (2004), 'Surface study of the corrosion of carbon steel in solutions of ammonium salts using Mössbauer Spectrometry', J. Radioanal. Nucl. Chem. Vol. 261, No.3, pp.593-596.

Wan, Y., Yan, C. (2003),'characterization of the rust on carbon steels pre-corroded by different gaseous pollutants', Journal of Materials Science, Vol. 38, pp.3597-3602.

ISSN 1466-8858 Volume 14, Preprint 4 submitted 5 January 2011

Freire, L., Nóvoa, X.R., Montemor, M.F., Carmezim, M.J. (2009), 'Study of passive films formed on mild steel in alkaline media by the application of anodic potentials', Materials Chemistry and Physics, Vol. 114, No.2, pp.962–972.

Benmoussa, A., Hadjel, M., Traisnel, M. (2009), 'Corrosion behavior of API 5L X-60 pipeline steel exposed to near-neutral pH soil simulating solution', Material and Corrosion, Vol. 57, No.10**,** pp.771 – 777.

McGannon, H.E. (1971), 'The Making, Shaping and Treating of Steel', 9th edn, 333, Pittsburgh, Pennsylvania, United States Steel.

Higgins, R.A. (1993), 'Engineering metallurgy', applied physical metallurgy, 6th. Edn, Arnold International Student Edition, London.

Samuels, L.E. (1980), 'Optical Microscopy of Carbon Steels', American Society for Metals, Metals Park, Ohio.

Stern, M., Geary, A. L. (1957), 'Electrochemical Polarization: I. A Theoretical Analysis of the Shape of Polarization Curves', J. of Electrochemical Society, Vol. 104, No. 1, pp.56-63

Zhong C., Tang X., Cheng Y.F. (2008), 'Corrosion of steel under the defected coating studied by localized electrochemical impedance spectroscopy', Electrochimica Acta, Vol.53, No.14, pp.4740-4747.

Raman, A., Kuban, B., Razvan , A. (1991), 'The application of infrared spectroscopy to the study of atmospheric rust systems', Corrosion Science, Vol. 32, No. 12, pp.1295-1306.

Misawa, T., Asami, K., Hshimoto, K., Shimodaira, S. (1974), 'The mechanism of formation of iron oxides and oxyhydroxides in aqueous solutions at room temperature', Vol 14, pp.131-149.

Yamashita, M., et al. (1994), 'The long term growth of the protective rust layer formed on weathering steel by atmospheric corrosion during a quarter of a century', Corrosion Science, Vol. 36, No. 2, pp.283-299.

ISSN:1466-8858 Volume 14, Preprint 1 Submitted 5 January 2011

Nishimura, T., Katayama, et al (2000), 'Electrochemical Behavior of Rust Formed on Carbon Steel in a Wet/Dry Environment Containing Chloride Ions', Corrosion, Vol.56, p.936.

Marco, J.F., et al. (2000), 'Characterization of the corrosion products formed on carbon steel after exposure to the open atmosphere in the Antarctic and Easter Island', Corrosion Science, Vol. 42, pp.753-771.

Oh, S. J., Cook, D. C., Townsend, H. E. (1999), 'Atmospheric corrosion of different steels in marine, rural and industrial environments', Corrosion Science, Vol. 41, pp.1687-1702.

Wan, y., Yan, C., Tan, J., Cao, C. (2004), 'Atmospheric Corrosion of Carbon Steels Pre-Corroded by Pollutants', Vol. 55, pp.119-123.

Cheng, Y.F. Luo, J.L. (1999), 'Passivity and pitting of carbon steel in chromate solutions', Electrochimica Acta, Vol. 44, pp.4795–4804.

Tiana, B.R., Cheng, Y.F. (2008), 'Electrochemical corrosion behavior of X-65 steel in the simulated oil sand slurry', Corrosion Science, Vol. 50, pp.773–779.

Cheng, Y.F. (2005), 'Studies of X-65 Pipeline Steel Corrosion in Solutions Containing Carbon Dioxide by Electrochemical Technique', Bulletin of Electrochemistry, Vol. 21, p. 503.

Asher, S.L., et al. (2007), 'Investigating a Mechanism for Transgranular Stress Corrosion Cracking on Buried Pipelines in Near-neutral pH Environments', Corrosion, Vol.63, p.932.

Du, C.W., et al. (2009), 'Effects of Microstructure on Corrosion of X70 Pipe Steel in an Alkaline Soil', J. of Materials Engineering and Performance, Vol. 18, 2, pp.216–220.

Bulger, J. et al. (2006),' Microstructural effect on near-neutral pH stress corrosion cracking resistance of pipeline steels', J. of Materials Science, vol. 41, pp.5001–5005.

Clover, D., Kinsel, B., et al. (2005), 'The influence of microstructure on the corrosion rate of various carbon steels', Journal of Applied Electrochemistry, Vol.3, pp.139–149.